Available online at www.sciencedirect.com
ScienceDirect
Journal of the European Ceramic Society 26 (2006) 3393–3397
www.elsevier.com/locate/jeurceramsoc

Microstructure and properties of Al_2O_3–TiC nanocomposites fabricated by spark plasma sintering from high-energy ball milled reactants

Yanfeng Zhang, Lianjun Wang, Wan Jiang *, Lidong Chen, Guangzhao Bai

State Key Laboratory of High Performance Ceramics and Superfine Microstructure, Shanghai Institute of Ceramics, Chinese Academy of Sciences, 1295 Dingxi Road, Shanghai 200050, China

Received 9 June 2005; received in revised form 27 August 2005; accepted 3 September 2005
Available online 24 October 2005

Abstract

In situ synthesis of Al_2O_3–TiC nanocomposite powders from a mixture of titanium, graphite, and Al_2O_3 powders by high-energy ball milling (HEBM) and its consolidation through spark plasma sintering (SPS) were investigated. After being milled for 25 h at ambient temperature, the powder mixtures were mainly composed of homogeneous nanosized Al_2O_3 particle and amorphous TiC solid solution. The relative density of the samples consolidated by SPS technique in vacuum at 1480 °C for 4 min reached 99.2%. The final products exhibited very fine microstructure, and the grain sizes of Al_2O_3 and TiC were about 400 nm and 200 nm, respectively, with a flexure strength of 944 ± 21 MPa, Vickers hardness 21.0 ± 0.3 GPa, fracture toughness 3.87 ± 0.2 MPa $m^{1/2}$, and electrical conductivity 1.2787×10^5 S m^{-1}.

Keywords: Al_2O_3–TiC; Milling; Nanocomposites; Mechanical properties; SPS

1. Introduction

Al_2O_3–TiC composites are widely used as substrate of magnetic heads and cutting tools due to their attractive mechanical properties and good electrical conductivity.[1] At present commercially available microsized Al_2O_3–TiC composites are prepared by pressureless sintering or hot pressing the direct mixtures of Al_2O_3 and TiC powders,[2,3] during which severe grain coarsening and generation of metal oxides at the interface[4] always take place due to relatively long holding time at high temperature. Because the binding force at the interface is not strong, grains are often pulled out when the Al_2O_3–TiC composites are being machined. It is especially detrimental if the grain size is large, which results in low product yield and then high manufacturing cost. Furthermore, the problem becomes more serious with the ongoing miniaturization of magnetic disk drive sliders. It is a current trend to prepare fine-grained Al_2O_3–TiC composites for future development of hard disk drive, moreover the reduction of grain size will result in improved properties.

High-energy ball milling machine (HEBM) has proved to be a powerful technique for synthesizing metal-metalloid compounds and fabricating homogeneously distributed nanocrystalline composites at ambient temperature.[5,6] Mechanically induced self-sustaining synthesis of monolithic nanocrystalline TiC powders and nanocrystalline TiC-contained composite powders via HEBM have been investigated by several researchers.[7–16]

SPS technique is an effective sintering process that allows densification of ceramics at a relatively lower temperature with short holding time owing to rapid heating and cooling rates. Recently, it has been reported by co-workers that in situ synthesis and sintering of submicron TiC/SiC composites,[17] Ti_5Si_3–TiC–Ti_3SiC_2 and Ti_5Si_3–TiC nanocomposites,[18] and TiC/SiC nanocomposites[19,20] through SPS technique were successfully carried out.

In the present paper, Al_2O_3–TiC nanocomposite powders were in situ synthesized from elemental Ti, C and Al_2O_3 powders by HEBM, and then the as-milled reactants were consolidated into fully dense nanostructured Al_2O_3–TiC composites by SPS, and finally the properties of the as-sintered sample were investigated.

2. Experimental procedure

The raw materials used in this work were 99.5% pure titanium powder (−325 mesh, Shanxi Bongen Titanium Co. Ltd., Shanxi,

* Corresponding author. Tel.: +86 21 52411118; fax: +86 21 52413122.
E-mail address: wanjiang@mail.sic.ac.cn (W. Jiang).

0955-2219/$ – see front matter © 2005 Elsevier Ltd. All rights reserved.
doi:10.1016/j.jeurceramsoc.2005.09.036

China), 99.9% pure graphite powder (−325 mesh, Shanghai Carbon Materials Factory, Shanghai, China) and 99.9% pure alumina (average particle size of 300 nm, Shanghai Wusong Chemical Factory, Shanghai, China). Titanium and graphite powders with a molar ratio 1:0.95 were mixed with Al_2O_3 powder to yield a TiC content 40 wt.% in the end-product. The mixed powders were put into the vial of high-energy ball milling machine (Model GN-2, Shengyang Science Equipment Factory, Shengyang, China). The milling was conducted using a serial of hardened steel balls. The ball-to-powder weight ratio was 13:1, and the steel vial was sealed in a glove box under argon atmosphere, with a milling speed at 480 rpm. The milling was interrupted per 5 h to inspect for sticking, and to scrape off the powders if necessary. A small amount of the powders were also collected after selected milling times in Ar gas to evaluate the progress of milling. The collected powders were analyzed by XRD (Cu Kα radiation). Particle morphology observation and crystal structure determination were performed using TEM with selected area electron diffraction (SAD).

The as-milled powders were put into a graphite die (15 mm in diameter), and graphite sheets were inserted into the inside of die in order to prevent the reaction between the powders and the die during sintering process. The samples were sintered with Dr. Sinter® 2040 spark plasma sintering system (Sumitomo Coal Mining Co., Tokyo, Japan) in vacuum (less than 4 Pa). The heating rate was about 50 °C/min and the pressure was applied at final stage of sintering process and maintained constant at 50 MPa. The temperature was held at 1480 °C for 4 min before turning off the power.

Both surfaces of the as-prepared samples were ground to remove the graphite layer and then analyzed by XRD. The densities of consolidated specimens were obtained using the Archimedes' immersion method with deionized water as the immersion medium. The theoretical densities of the specimens were calculated according to mixture rule. Microstructural observation was conducted using SEM and TEM. The samples were machined to 1 mm × 1.3 mm × 12 mm bars for measuring the three-point bending strength (σ_b) with a span of 10 mm. For each material six beams were tested. Vickers hardness (H_v) and fracture toughness (K_{IC}) were measured by indentation technique (Wilson-wolpert Tukon® 2100B). The indentation parameters were made using 5-kg load with a dwell of 10 s. A half-penny crack was found after indentation. Six normal values of crack length were obtained and then the following equation was used to calculate the fracture toughness[21]:

$$K_{IC} = 0.016\left(\frac{E}{H_v}\right)^{1/2}\left(\frac{P}{c^{3/2}}\right) \quad (1)$$

where E, H_v, P and c refer to Young's modulus, Vickers hardness, the applied indentation load, and the half-length of the radial crack, respectively. The modulus E has been reported to increase nearly linearly with increasing TiC content in the range of 0–40 mass%.[22] According to this relation, as $E(Al_2O_3) = 393$ GPa and $E(TiC) = 460$ GPa, we had $E(Al_2O_3/40\ mass\%TiC) = 416$ GPa. The electrical conductivity (σ) of sintered bodies was measured by four-probe method.[23]

3. Results and discussion

The XRD patterns of ball milled powder mixtures after selected times are presented in Fig. 1a–e. Sharp peaks of elemental Ti and C can be seen in Fig. 1a, which is the XRD pattern of the starting powder mixtures. After milling 10 h, the peaks of graphite disappear completely, while the peaks of titanium are still visible, with the intensities decreasing and the widths broadening, which mean the refinement of Ti grains. The disappearance of graphite is due to a solid state diffusion of the C atoms into the grain boundaries and defects of Ti particles, and to the high absorption coefficient of the fine graphite particles,[7–9] but there are barely reactions between Ti and C, which can be supported by the fact that no TiC phase is detected by XRD. After milling 15 h, the diffractions of TiC appear, as is shown in Fig. 1c. After milling 20 h, the peaks of Ti almost vanish and at the same time the peaks of TiC become obvious. Further milling to 25 h leads to the slight decrease in strength and increase in width of the diffraction peaks of TiC, which indicates that most of the elemental Ti and C have converted into poorly crystallined or even amorphouse TiC solid solution after milling 20 h. It should be mentioned that during the whole ball milling process the Al_2O_3 grains refine continually without phase transformation. The XRD pattern of Al_2O_3–TiC nanocomposites consolidated at 1480 °C for 4 min under 50 MPa by spark plasma sintering is shown in Fig. 1f. As can be seen, the diffraction peaks of both Al_2O_3 and TiC increase remarkably in comparison with that of Fig. 1e, meaning that the initially amorphous TiC solid solution is crystallized and that fine Al_2O_3 grains grow. According to the Scherrer equation, the average grain sizes of Al_2O_3 and TiC are 329 nm and 210 nm, respectively. No impurity phase can be seen in Fig. 1f, which means no unexpected reaction occurs.

The TEM micrograph of the powder mixtures milled for 25 h and corresponding selected area electron diffraction (SAD) pattern are shown in Fig. 2. It is difficult to distinguish and estimate the grain size of both Al_2O_3 and TiC by direct observation of TEM image because they are poorly crystallized or amorphous. The corresponding SAD pattern in the right lower corner of Fig. 2 shows bright continuous diffraction rings of TiC indi-

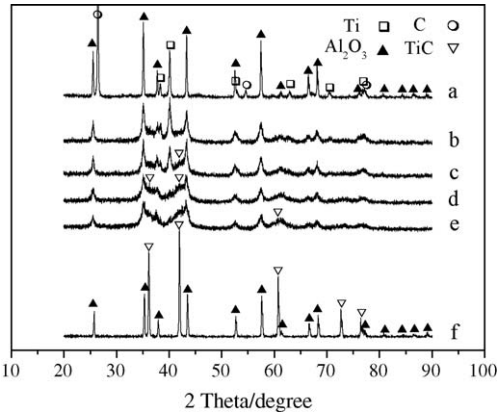

Fig. 1. XRD patterns of the collected powders after different milling periods and the as-prepared product: (a) 0 h; (b) 10 h; (c) 15 h; (d) 20 h; (e) 25 h; (f) 25 h of milling followed by SPS at 1480 °C for 4 min under 50 MPa.

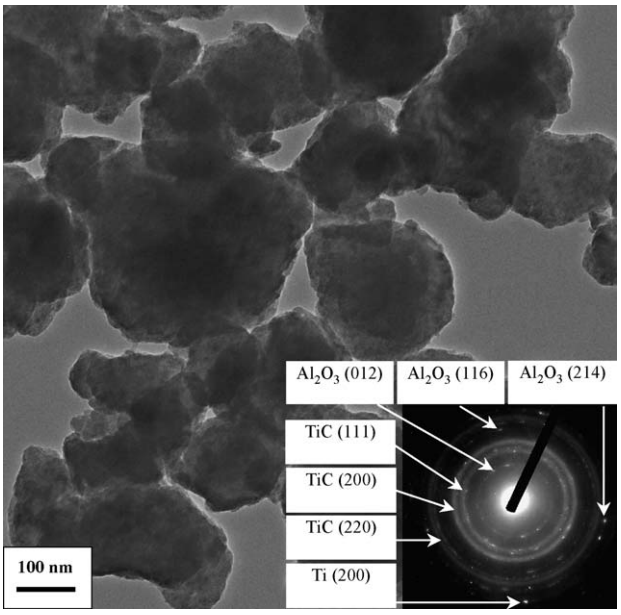

Fig. 2. TEM micrograph of powder mixtures milled for 25 h and corresponding selected area electron diffraction (SAD) pattern. Bright continuous diffraction rings of TiC indicate yielding of a large quantity of TiC particles during ball milling process.

cating yielding of a large quantity of TiC solid solution during ball milling process. Relatively darker discontinuous diffraction rings of Al_2O_3 imply that the particles are poorly crystallized or amorphousized, and some diffraction spots of Ti imply existence of unreacted elemental Ti. Therefore the final powder mixtures consist of amorphous TiC solid solution, nanophase Al_2O_3 and a small amount of unreacted nanosized Ti and C particles.

Fig. 3 shows the backscattered SEM image of polished Al_2O_3–TiC bulk sample fabricated by SPS. The gray-white phase is the TiC, and the dark phase is the Al_2O_3 matrix. It is shown that the fine TiC particles are homogeneously distributed in the Al_2O_3 matrix. No pore can be seen in the polished surface, which demonstrates that the sintered body has been fully

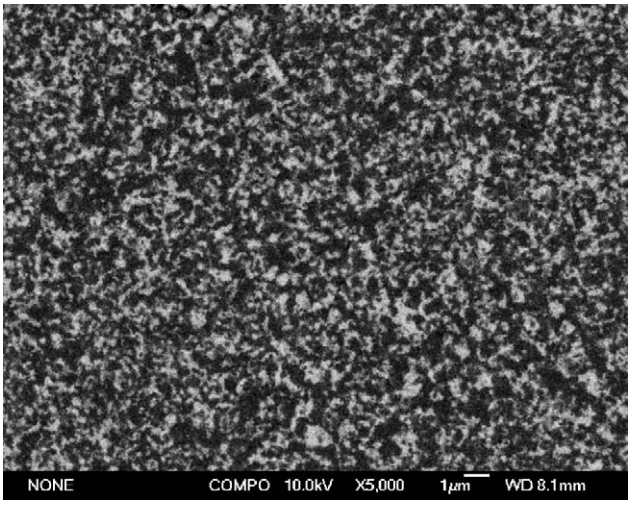

Fig. 3. Backscattered SEM image of polished surface of the sintered sample. The gray-white phase is the TiC, and the dark phase is the Al_2O_3 matrix.

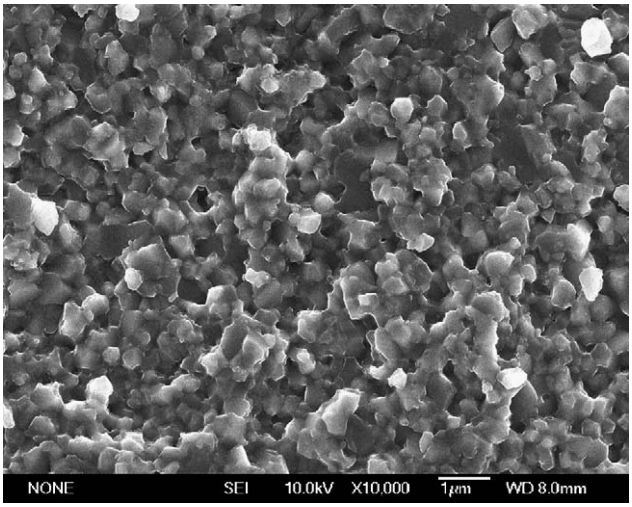

Fig. 4. SEM micrograph of fracture surface of the sintered sample.

densified by SPS. The density of the as-sintered sample reaches 99.2% of the theoretical density.

Fig. 4, SEM micrograph of the fracture surface of the sintered sample, clearly shows that the microstructure is composed of fine Al_2O_3 and TiC grains with the grain size less than 500 nm, moreover, the grain sizes distribution is narrow. In addition, it is easy to see that the fracture mode of the sintered sample is primarily intergranular.

As is shown in Fig. 5, TEM analysis is conducted to further study the microstructure of the sintered sample. Most of TiC and Al_2O_3 grains confirmed by electron diffraction patterns are very fine, and the average grain sizes of TiC and Al_2O_3 are about 200 nm and 400 nm, respectively, corresponding with the above obtained result from the Scherrer equation.

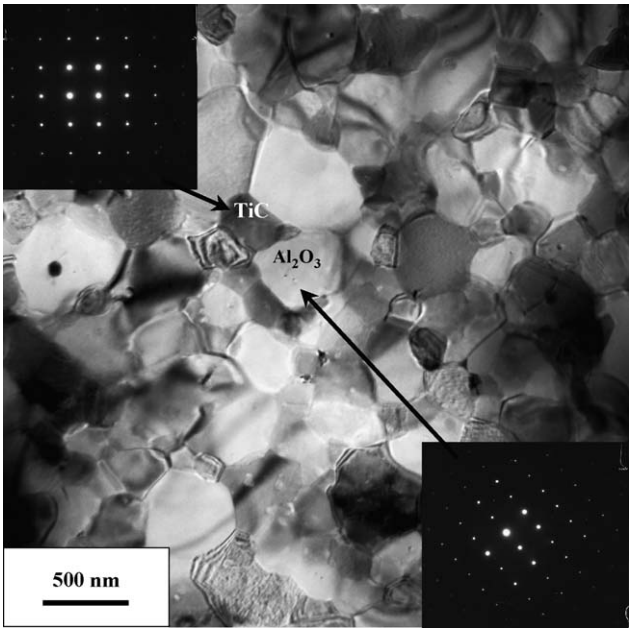

Fig. 5. TEM image of the sintered sample with electron diffraction patterns of Al_2O_3 and TiC.

Table 1
Mechanical properties and electrical conductivity of the sintered sample

No.	Raw materials	Fabrication method	Relative density	Grain size (μm)		Mechanical properties			Electrical conductivity
						σ_b (MPa)	H_v (GPa)	K_{IC} (MPa m$^{1/2}$)	σ (10^5 S m^{-1})
1	Al_2O_3, Ti, C	*HSPS	99.2%	Al_2O_3 TiC	0.4 0.2	944 ± 21	21.0 ± 0.3	3.87 ± 0.20	1.279
2	Al_2O_3, TiC	*WHP	98.4%	Al_2O_3 TiC	0.9 0.5	785 ± 86	20.7 ± 0.9	4.27 ± 0.45	0.163

No. 1 sample: Al_2O_3 + 40 wt.%TiC (35 vol%TiC); *HSPS: high-energy ball milling + SPS; No. 2 sample[22]: Al_2O_3 + 30 vol%TiC; *WHP: wet milling + hot-pressing sintering.

Mechanical properties and electrical conductivity of the sintered specimens are listed in Table 1. It can be seen that the Al_2O_3–TiC composites prepared by in situ reaction have finer microstructure and higher relative density than the hot-pressed sample. The refinement of microstructure is attributable to improvement of strength[24] and to the reduction of the critical flaw size that is also beneficial for improvement of strength, so the strength of in-reacted synthesized sample is much higher than that of the hot-pressed sample, as shown in Table 1. The microstructural refinement does not lead to remarkable increase in hardness but lead to slightly decrease in fracture toughness. The fracture toughness of the monolithic Al_2O_3 decreases with reduction of grain size.[24] It was reported that the K_{IC} value of monolithic Al_2O_3 with a grain size of 350 nm was only 3.3 ± 0.14 MPa m$^{1/2}$,[25] in comparison with which the fracture toughness of the in situ synthesized Al_2O_3–TiC composites has been improved to 3.87 ± 0.20 MPa m$^{1/2}$.

The electrical conductivity of the in situ synthesized sample is almost an order of magnitude higher than that of hot-pressed one. The primary reason is that the homogeneously distributed electrically conductive TiC phase (2×10^6 S m^{-1}) in the in situ synthesized sample forms a more continuous electrically conductive network within the insulating Al_2O_3 phase (2×10^{-13} S m^{-1}). Furthermore the clean interface between in-situ reacted TiC grains also improved the electrical conductivity. Additionally a slightly higher content of TiC phase in the in situ synthesized sample is also responsible for the improvement of electrical conductivity.

4. Conclusions

The Al_2O_3–TiC nanocomposite powder has been synthesized by HEBM, and subsequently was densified by SPS. HEBM leads to a large amount of nano-sized Al_2O_3–TiC nanocomposite powder, which showed excellent sinterablity. Near fully dense and fine-grained Al_2O_3–TiC composites fabricated by SPS exhibit excellent comprehensive properties.

Acknowledgments

This work was supported by the National Natural Science Foundation of China (50302012 and 50232020) and the Open Foundation of State Key Laboratory (No.SKL200504SIC).

References

1. Xia, T. D., Munir, Z. A., Tang, Y. L., Zhao, W. J. and Wang, T. M., Structure formation in the combustion synthesis of Al_2O_3-TiC composites. *J. Am. Ceram. Soc.*, 2000, **83**, 507–512.
2. Burden, S. J., Hong, J., Rue, J. W. and Stromsborg, C. L., Comparison of hot-isostatically-pressed and uniaxially hot-pressed alumina-titanium-carbide cutting tools. *Ceram. Bull.*, 1988, **67**, 1003–1005.
3. Cutler, R. A., Hurford, A. C. and Virkar, A. V., Pressureless-sintered Al_2O_3-TiC composites. *Mater. Sci. Eng.*, 1988, **A105–106**, 183–192.
4. Kim, Y. W. and Lee, J. G., Pressureless Sintering of alumina-titanium carbide composites. *J. Am. Ceram. Soc.*, 1989, **72**(8), 1333–1337.
5. Zhang, D. L., Processing of advanced materials using high-energy mechanical milling. *Prog. Mater. Sci.*, 2004, **49**, 537–560.
6. Takacs, L., Self-sustaining reactions induced by ball milling. *Prog. Mater. Sci.*, 2002, **47**, 355–414.
7. Liu, Z. G., Ye, L. L., Guo, J. T., Li, G. S. and Hu, Z. Q., Self-propagating high-temperature synthesis of TiC and NbC by mechanical alloying. *J. Mater. Res.*, 1995, **10**, 3129–3535.
8. Liu, Z. G., Guo, J. T., Ye, L. L., Li, G. S. and Hu, Z. Q., Formation mechanism of TiC by mechanical alloying. *Appl. Phys. Lett.*, 1994, **65**(21), 2666–2668.
9. Ye, L. L. and Quan, M. X., Synthesis of nanocrystalline TiC powders by mechanical alloying. *Nanostruct. Mater.*, 1995, **5**(1), 25–31.
10. Ye, L. L., Liu, Z. G., Quan, M. X. and Hu, Z. Q., Different reaction mechanisms during mechanical alloying $Ti_{50}C_{50}$ and $Ti_{33}C_{67}$. *J. Appl. Phys.*, 1996, **80**, 1910–1912.
11. Wu, N. Q., Lin, S., Wu, J. M. and Li, Z. Z., Mechanosynthesis mechanism of TiC powders. *Mater. Sci. Technol.*, 1998, **14**, 287–291.
12. El-Eskandarany, M. S., Structure and properties of nanocrystalline TiC full-density bulk alloy consolidated from mechanically reacted powders. *J. Alloys Compd.*, 2000, **305**, 225–238.
13. Zhu, X. K., Zhao, K. Y., Cheng, B. C., Lin, Q. S., Zhang, X. Q., Chen, T. L. and Su, Y. S., Synthesis of nanocrystalline TiC powder by mechanical alloying. *Mater. Sci. Eng.*, 2001, **C16**, 103–105.
14. Li, J. L., Li, F. and Hu, K. A., Formation of titanium carbide/aluminum oxide nanocomposite powder by high-energy ball milling and subsequent heat treatment. *J. Am. Ceram. Soc.*, 2002, **85**, 2843–2845.
15. Li, J. L., Li, F., Hu, K. A. and Zhou, Y., TiB_2/TiC nanocomposite powder fabricated via high energy ball milling. *J. Eur. Ceram. Soc.*, 2001, **21**, 2829–2833.
16. Lee, J. W., Munir, Z. A. and Ohyanagi, M., Dense nanocrystalline TiB_2/TiC composites formed by field activation from high-energy ball milled reactants. *Mater. Sci. Eng.*, 2002, **A325**, 221–227.
17. Wang, L. J., Jiang, W., Chen, L. D. and Bai, S. Q., Rapid reactive synthesis and sintering of submicron TiC/SiC composites through spark plasma sintering. *J. Am. Ceram. Soc.*, 2004, **87**(6), 1157–1160.
18. Wang, L. J., Jiang, W. and Chen, L. D., Microstructure of Ti_5Si_3-TiC-Ti_3SiC_2 and Ti_5Si_3-TiC nanocomposites in-situ synthesized by spark plasma sintering (SPS). *J. Mater. Res.*, 2004, **19**, 3004–3008.

19. Wang, L. J., Jiang, W. and Chen, L. D., Fabrication and characterization of nano-SiC particles reinforced TiC/SiC nanocomposites. *Mater. Lett.*, 2004, **58**(9), 1401–1404.
20. Wang, L. J., Jiang, W. and Chen, L. D., Rapidly sintering nanosized SiC particle reinforced TiC composites by the spark plasma sintering (SPS) technique. *J. Mater. Sci.*, 2004, **39**, 4515.
21. Antis, G. R., Chantikul, P., Lawn, B. R. and Marshall, D. B., A critical evaluation of indentation techniques for measuring fracture toughness: I, Direct crack measurements. *J. Am. Ceram. Soc.*, 1981, **64**(9), 533–538.
22. Wahi, R. P. and Ilschner, B., Fracture behaviour of composites based on Al_2O_3-TiC. *J. Mater. Sci.*, 1980, **15**, 875–885.
23. Bellosi, A., Portu, G. D. and Guicciardi, S., Preparation and properties of electroconductive Al_2O_3-based composites. *J. Eur. Ceram. Soc.*, 1992, **10**, 307–315.
24. Rice, R. W., *Mechanical Properties of Ceramics and Composites: Grain and Particles Effects*. Marcel Dekker, Inc., New York, 2000.
25. Zhan, G. D., Kuntz, J., Wan, J., Garay, J. and Mukherjee, A. K., Spark-plasma-sintered $BaTiO_3/Al_2O_3$ nanocomposites. *Mater. Sci. Eng.*, 2003, **A356**, 443–446.